



HAL
open science

Trapping and adsorption of CO in amorphous ice: a FTIR study

O. Óscar Gálvez, Belén Maté, Víctor J. Herrero, Rafael Escribano

► **To cite this version:**

O. Óscar Gálvez, Belén Maté, Víctor J. Herrero, Rafael Escribano. Trapping and adsorption of CO in amorphous ice: a FTIR study. *Icarus*, 2008, 197 (2), pp.599. 10.1016/j.icarus.2008.05.016 . hal-00499087

HAL Id: hal-00499087

<https://hal.science/hal-00499087>

Submitted on 9 Jul 2010

HAL is a multi-disciplinary open access archive for the deposit and dissemination of scientific research documents, whether they are published or not. The documents may come from teaching and research institutions in France or abroad, or from public or private research centers.

L'archive ouverte pluridisciplinaire **HAL**, est destinée au dépôt et à la diffusion de documents scientifiques de niveau recherche, publiés ou non, émanant des établissements d'enseignement et de recherche français ou étrangers, des laboratoires publics ou privés.

Accepted Manuscript

Trapping and adsorption of CO₂ in amorphous ice: a FTIR study

Óscar Gálvez, Belén Maté, Víctor J. Herrero, Rafael Escribano

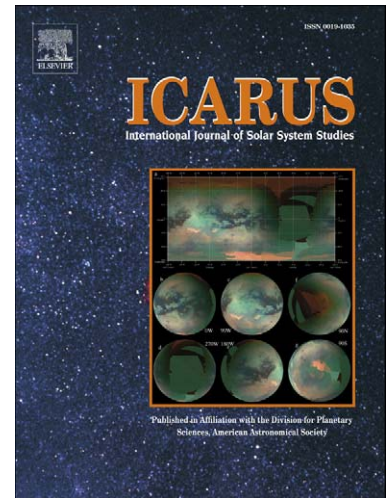
PII: S0019-1035(08)00218-2
DOI: [10.1016/j.icarus.2008.05.016](https://doi.org/10.1016/j.icarus.2008.05.016)
Reference: YICAR 8696

To appear in: *Icarus*

Received date: 12 February 2008
Revised date: 30 April 2008
Accepted date: 19 May 2008

Please cite this article as: Ó Gálvez, B. Maté, V.J. Herrero, R. Escribano, Trapping and adsorption of CO₂ in amorphous ice: a FTIR study, *Icarus* (2008), doi: 10.1016/j.icarus.2008.05.016

This is a PDF file of an unedited manuscript that has been accepted for publication. As a service to our customers we are providing this early version of the manuscript. The manuscript will undergo copyediting, typesetting, and review of the resulting proof before it is published in its final form. Please note that during the production process errors may be discovered which could affect the content, and all legal disclaimers that apply to the journal pertain.



Trapping and adsorption of CO₂ in amorphous ice: a FTIR study

Óscar Gálvez, * Belén Maté, Víctor J. Herrero, and Rafael Escribano

Instituto de Estructura de la Materia, CSIC, Serrano 121-123, 28006, Madrid, Spain

*Corresponding Author E-mail address: ogalvez@iem.cfmac.csic.es

Pages: 31

Figures: 4

Tables: 2

Proposed running head: Trapping and adsorption of CO₂ in amorphous ice: a FTIR study

Editorial correspondence to:

Dr. Óscar Gálvez

Instituto de Estructura de la Materia, CSIC

Serrano 123, 28006,

Madrid, Spain

Phone: +34 91 5616800 ext. 1120

Fax: +34 91 5855184

E-mail address: ogalvez@iem.cfmac.csic.es

Abstract

The interaction of carbon dioxide and amorphous water ice at 95 K is studied using transmission infrared spectroscopy. Samples are prepared in two ways: co-deposition of the gases admitted simultaneously or sequential deposition, in which amorphous water ice (ASW) is grown first and CO₂ vapour is added subsequently. In either case, a fraction of the CO₂ molecules is found to interact with water in a way that gives rise to shifts and splittings in the infrared bands with respect to those of a pure CO₂ solid. In co-deposition experiments, a larger amount of carbon dioxide is trapped within the amorphous water than in sequential deposition samples, where a substantial proportion of molecules appears to be trapped in macropores of the ASW. The specific surface area of sequential samples is evaluated and compared to previous literature results. When the sequential samples are heated to 140 K, beyond the onset temperature at which water ice undergoes a phase transition, the CO₂ molecules at the pores relocate inside the bulk in a structure similar to that found in co-deposited samples, as deduced by changes in the shape of the CO₂ infrared bands.

Keywords: *CO₂, H₂O, intermolecular interaction, amorphous water ice, trapping, adsorption*

1. Introduction.

Amorphous water ice, commonly referred to as amorphous solid water (ASW), is a metastable form of ice and the most abundant component of the molecular ices observed in the interstellar medium (Williams et al., 2007). Although ASW has been studied for many years, there are often discrepancies among the diverse literature results describing its physical properties. In particular, disagreement appears in the published values of specific surface area (total surface area divided by the mass of the solid), SSA, with values ranging from 10 to more than $200 \text{ m}^2\text{g}^{-1}$ reported in different works (see e.g. discussions in Mayer and Pletzer, 1986, or Manca et al., 2003). Temperature values of phase conversion of ASW to cubic ice also show large discrepancies. For example Hagen et al. (1981) give a value around 130 K, Bar-Nun et al. (1987) ~ 140 K, Boxe et al. (2007) 150 K, and Kumi et al. (2006) around 155 K. Such differences are due to the fact that the amorphous ice properties depend on the way the ice is prepared: e.g. growing conditions or thermal history (Kimmel et al., 2001; Jenniskens and Blake, 1994).

Different molecules such as CO, CO₂, CH₃OH, NH₃, CH₄, etc. are often present in the ASW found in space (e.g. Dartois, 2005; Gerakines et al., 2005; and references therein). Mixed ices of CO₂ and water are known to be present, for example, in the frozen nuclei of comets (Crovisier, 2006), in various satellites of our solar system (e.g. Grundy et al., 2003; Buratti et al, 2005), and as components of dust interstellar particles (e.g. Strazzulla et al, 1998; Draine 2003). Prompted by these findings, solid H₂O/CO₂ ice mixtures, as laboratory analogues of astrophysical objects, have been studied for many years, mainly by infrared spectroscopy and mass spectrometry, in temperature programmed desorption (TPD) experiments (see e.g. Sandford and Allamandola, 1990;

Ehrenfreund et al., 1999; Bernstein et al., 2005; Kumi et al., 2006; Malyk et al., 2007). In two recent publications (Gálvez et al., 2007; Maté et al., 2008), our group has presented FTIR transmission and reflection-absorption (RAIR) spectra of ices of CO₂ and water prepared by sequential deposition or co-deposition of these species, detecting spectral variations which may characterize two different structures or kinds of association between carbon dioxide and water, either of which may be dominant depending on the temperature and deposition scheme. These spectral variations have been observed before in investigations carried out under different conditions (Sandford and Allamandola, 1990; Kumi et al., 2006). The two different CO₂ structures have been labeled (Maté et al., 2008; Gálvez et al., 2007) CO₂-ext and CO₂-int, for external and internal respectively. The meaning of these terms is the following: in CO₂-ext the interaction between CO₂ and water is quite weak, as it would be if CO₂ were superficially adsorbed, for instance, whereas by internal it is meant that the CO₂ molecules enter the bulk of ASW. It was found in these studies that CO₂-ext in a H₂O/CO₂ ice mixture presents some similar characteristics to those of a pure CO₂ crystal. Both desorb at nominal temperatures around 90-110 K and show a strong peak in the IR spectra at $\sim 2343\text{-}2344\text{ cm}^{-1}$ at 80 K (Gálvez et al., 2007). On the other hand, CO₂-int displays a specific behaviour in some physical properties, which indicate that in this case the CO₂ molecules are subject to different intermolecular interactions than those present in a pure CO₂ crystal. The desorption of CO₂-int is entirely controlled by the ASW, taking place between 155 and 168 K, the interval where faster crystallization rates from ASW to I_c have been observed (Jenniskens and Blake, 1994). The major peak in the FTIR spectra is shifted to $\sim 2340\text{ cm}^{-1}$, a lower frequency than that of pure CO₂ or CO₂-ext.

As mentioned above, two previous papers of our group presented investigations on the carbon dioxide/water system from different points of view and methodology. Gálvez et al., 2007, used transmission IR spectroscopy and TPD experiments to characterize the existence of the two CO₂ structures indicated above, giving also activation energies for the desorption of CO₂ from amorphous and crystalline water ice. In a further work, Maté et al., 2008, employed RAIR spectroscopy to study the morphology and temperature alterations of samples generated by four different deposition techniques, and performed theoretical calculations of a pure CO₂ crystal, with a comparison of theoretical and experimental results. In the present work, we focus on the growing process of CO₂-int in H₂O/CO₂ ice mixtures and its dependence on temperature and deposition procedure of CO₂. We quantify the amount of CO₂-int formed by codeposition and sequential deposition schemes, and provide a value for the specific surface area of ASW at 95 K using CO₂ as probe molecule, for the first time within our knowledge. Also, we carry out a study of the temperature evolution of these systems in the range between 95 and 165 K, providing evidence on changes in the CO₂ distribution in ASW when phase changes take place.

2. Experimental section

Our experimental set-up has been described in detail before (Carrasco et al., 2002; Maté et al., 2003; Gálvez et al., 2007). In brief, it consists of a high vacuum cylindrical chamber, evacuated by a turbomolecular pump. The chamber has a liquid nitrogen Dewar flask in contact with a 1 mm thick deposition substrate made of Si. The background pressure in the chamber is usually in the 10⁻⁸ mbar range. The chamber is coupled to a Fourier transform infrared spectrometer (Bruker Vertex70) through a

purged pathway, with KBr windows for the incident and transmitted radiation, which is focused on exit onto a MCT detector. The substrate is mounted on a holder that allows temperature control, with about 1 K accuracy, between 80 and 250 K. Spectra were recorded with a nominal resolution of 2 cm^{-1} with 512 co-added scans for each spectrum. Controlled flows of CO_2 and water vapour were introduced through independent needle valves to backfill the chamber. Distilled water previously freeze-pump-thawed three times and 99.998 % purity CO_2 from Air Liquide were used in all the experiments. The main chamber is coupled, by means of a regulation valve, to a differentially pumped chamber containing an Inficon, Transpector 2 quadrupole mass spectrometer (QMS), which is used to monitor the vapor composition during the deposition process. This additional QMS chamber, already employed in our previous works on the $\text{CO}_2/\text{H}_2\text{O}$ system (Gálvez et al. 2007, Maté et al. 2008), is an improvement of our original configuration (Carrasco et al. 2002, Maté et al. 2003), intended to establish a pressure difference of up to two orders of magnitude between the deposition chamber and the QMS chamber. This modification allows the use of the QMS to control the vapor composition even for relatively high deposition pressures like some of those selected in the present work ($P > 5 \times 10^{-5}$ mbar). During all the experiments, the position of the regulation valve connecting the two chambers was kept fixed. The use of this two-chamber scheme requires a careful calibration of the QMS to avoid problems associated with the different efficiency of the turbomolecular pumps for molecules with different masses. The calibration of the QMS was performed by correlating absolute pressure values of water or CO_2 in the main chamber, with the corresponding QMS readings at $m/q=18$ and $m/q=44$. Absolute pressures were determined from the growing rates of the solid films on the substrates (Maté et al, 2003). The film thickness values, needed for the calculation of the growing rates, can be derived either from absorbance

values (Gálvez et al, 2007) in IR transmission experiments, or from interference patterns in reflection-absorption measurements (Maté et al, 2003). In the present work we have simulated our transmission spectra with the optical constants of Toon et al. (1994) for H₂O and of Ehrenfreund et al. (1997) for CO₂. The calibration of the QMS remained stable in the course of the current experiments as verified by periodic checks. The relative sensitivity of the QMS (without electron multiplier) for H₂O and CO₂ was found to correspond roughly to the ratio of the respective ionization cross sections. The estimated error in the absolute pressures is $\approx 10\%$. Deposition pressures ranged between approximately 5×10^{-7} and 5×10^{-5} mbar.

Films of H₂O/CO₂ ice were prepared by sequential deposition and co-deposition of the appropriate vapours on the substrate held at 95 K. This temperature, relevant for Solar System bodies, was chosen for experimental convenience. At this temperature, the CO₂ saturation pressure is in a range suitable to our experimental setup. In this work, the CO₂ pressure at which CO₂-ext starts to grow in the ice mixtures, i.e. the saturation pressure, is measured as 4.3×10^{-5} mbar and 6.6×10^{-5} mbar in sequential deposition and co-deposition experiments respectively. The CO₂/H₂O ratio in the ice was determined from the transmission infrared spectra. The amount of water deposited can be calculated from the integrated absorbance of the O-H stretching band. The column density of water molecules is obtained by using the band intensity given by Gerakines et al. (1995) for pure water ice at 80 K, $A = 2.1 \times 10^{-16}$ cm/molecule. Although a slight dependence of the OH-stretching band of water ice with CO₂ concentration has been reported in the literature (Öberg et al., 2007), we have neglected that variation due to the small amount of CO₂ present in our ice mixtures, less than 5 % in all cases. To determine the number of CO₂ molecules present in the ice we have followed a similar procedure. The integrated absorbance of the ν_3 band of CO₂ was converted to molecular column density

by means of the band intensity, $A = 7.1 \times 10^{-17}$ cm/molecule, given by Gerakines et al. (1995). This value corresponds to a binary ice mixture of H₂O/CO₂ in a ratio 24:1 at 10 K. The temperature affects ice properties and the A values could be slightly different at 95 K. Sandford and Allamandola (1990) estimated that the A value for the ν_3 band of CO₂ decreases around 0.5 % every 14 K temperature rise, which should not affect significantly our results. We have estimated a 5% error in our integrated areas, giving a 7% error in the corresponding $n_{\text{CO}_2}/n_{\text{H}_2\text{O}}$ ratios (n : number of molecules).

3. Results and discussion

Figure 1 presents a transmission IR spectrum of a H₂O/CO₂ co-deposited sample at 95 K with a calculated percentage of CO₂ in water of 4.5%. In addition to the broad O-H stretching, bending and libration bands of water at ~ 3230 , 1650 cm^{-1} and 800 cm^{-1} , respectively, narrow bands corresponding to the ν_3 and ν_2 modes of CO₂ are easily recognized at 2340 cm^{-1} and 656 cm^{-1} , respectively. A small peak at 2275 cm^{-1} can be also observed, assigned to the ν_3 band of ¹³CO₂. As it was mentioned in our previous studies (Gálvez et al., 2007; Maté et al., 2008), the main spectral features of CO₂-int in a H₂O/CO₂ mixture that differ from the spectrum of pure CO₂ crystals are: (1) a red shift of ~ 4 cm^{-1} of the ν_3 band (at ~ 2345 cm^{-1} in pure CO₂); (2) a corresponding shift of ~ 7 cm^{-1} of the same band of ¹³CO₂ (at ~ 2282 cm^{-1} in pure CO₂); (3) a broad structure in the ν_2 band (instead of the crystal-field splitting in a pure CO₂ crystal, with a double peak at ~ 661 and 655 cm^{-1}). These characteristics are visible in the samples analyzed in this study. Table 1 summarizes observed wavenumbers for the vibrational bands of CO₂-int from spectra of co-deposited CO₂/H₂O mixtures, recorded in this work and in previous publications, compared to pure CO₂ values. In the spectral region 3800 – 3500

cm^{-1} only a weak feature at 3696 cm^{-1} is observed. This band has been assigned by Roland and Devlin (1991) to the “dangling OH” of ASW. We do not detect any trace of CO_2 combination bands in the spectra of our co-deposited samples at 95 K, in contrast with e.g. the observations by Hodyss (2008) on co-deposited ices grown at 15 K.

[Figure 1]

[Table 1]

Co-deposition experiments

It is important to consider that at 95 K the sticking efficiency of CO_2 molecules on a weakly-interacting substrate like Si is close to zero, whereas the sticking coefficient for water at this temperature is one (Sandford and Allamandola, 1990). In other words, when a $\text{CO}_2/\text{H}_2\text{O}$ gas mixture is admitted into the chamber, there is a much lower probability to deposit CO_2 than water, although the presence of water favours the CO_2 condensation. Under these conditions, the presence of CO_2 molecules in the amorphous solid could be explained by the mechanism of gas trapping (e.g. Bar-Num et al., 2007). The basic idea is that, when water vapour freezes into the ASW structure in the presence of other gases, the guest gas molecules stick to the ice and reside there for a time which depends on the intermolecular interacting forces. If the pores or cavities of ASW are covered by additional water molecules before the guest gas molecules can escape, they remain trapped and can be released only upon a phase change of the solid.

The $\text{H}_2\text{O}:\text{CO}_2$ ratio of the ice mixtures can be varied by choosing different partial pressures of the gases during the co-deposition. We have selected in this investigation water pressures between 3.2×10^{-6} and 1.6×10^{-5} mbar, and CO_2 pressures

between 3.2×10^{-7} and 4.7×10^{-5} mbar. Working at constant water vapour pressure, ices were formed by varying the CO_2 pressure. Deposition times ranged between five and twenty minutes leading to ice thickness between 100 and 370 nm. Figure 2a shows the molecular ratio, $n_{\text{CO}_2}/n_{\text{H}_2\text{O}}$, in the ice mixture versus the CO_2 pressure, at constant $p_{\text{H}_2\text{O}}$. The $n_{\text{CO}_2}/n_{\text{H}_2\text{O}}$ ratio is estimated from the spectra as indicated above. The maximum CO_2 concentration was 5%, corresponding to the highest CO_2 pressure represented in Figure 2. At higher pressures CO_2 -ext begins to grow and the resulting ice samples have not been considered in the present study.

[Figure 2]

In co-deposition experiments, the trapping mechanism should be responsible for the presence of CO_2 in the amorphous ice, as ice formation and trapping are simultaneous processes. As shown in Figure 2a, the amount of CO_2 -int trapped depends on the partial pressures selected in the gas phase, and a non linear dependence with P_{CO_2} is observed. However, at very low CO_2 partial pressures ($< 5 \times 10^{-6}$ mbar) the amount of solid CO_2 is approximately proportional to its vapour partial pressure during co-deposition, as it was recently suggested (Malyk et al., 2007). All three series of measurements agree within their estimated uncertainties. However, slightly smaller values are obtained for the highest water pressure (solid triangles in Fig. 2a). This is consistent with the trapping mechanism, as a lower $\text{CO}_2:\text{H}_2\text{O}$ ratio is used for the vapours.

Sequential deposition experiments

We have also conducted a series of experiments with sequentially deposited $\text{H}_2\text{O}/\text{CO}_2$ ices (see Fig. 2b). Films of ASW were grown at 95 K and then exposed to

different CO₂ partial pressures, in all cases lower than the saturation value of 4.3x10⁻⁵ mbar, at which CO₂-ext starts to grow in these experiments. The CO₂ pressure was maintained for a few minutes until a constant infrared band was observed in the spectra. Two water deposition rates, 0.2 nm/s and 0.6 nm/s, corresponding to pressures of 5x10⁻⁶ mbar and 1.6x10⁻⁵ mbar respectively, were used to form water films of different thickness, always < 400 nm. Figure 2b shows the molecular ratio, $n_{\text{CO}_2}/n_{\text{H}_2\text{O}}$, versus partial pressure of CO₂, for three series of experiments. All three sets of data coincide within experimental error. The agreement for the results corresponding to the same deposition rate but different ice film thickness (circles and open boxes in Fig.2b) indicates that the number of CO₂ molecules that enter the solid per gram of water ice is constant. This behaviour is in accordance with the conclusions derived by Kumi et al. (2006), who found that the integrated absorbance of the residual ν_3 band of CO₂ varies linearly with ASW film thickness. The film grown at an approximately three times higher water deposition rate (solid triangles in Figure 2b) also admits a similar amount of CO₂-int. This result seems to indicate that the morphology of the ASW does not depend on the deposition rate, at least for the range of values of this work.

These sequential deposition experiments are similar to the standard adsorption isotherm experiments. The data in Fig. 2b follow a tendency that is usually assigned to a type II isotherm, typical of gases physisorbed on a solid (Rouquerol et al., 1999). This kind of isotherm is well described using the Brunauer, Emmet and Teller (BET) model (Brunauer et al., 1938). The BET isotherm model can be formulated as:

$$\frac{p_{\text{CO}_2}}{v(p_{\text{CO}_2}^0 - p_{\text{CO}_2})} = \frac{1}{v_m c} + \frac{c-1}{v_m c} \frac{p_{\text{CO}_2}}{p_{\text{CO}_2}^0}, \quad (1)$$

where p_{CO_2} is the actual pressure of CO_2 , $p_{CO_2}^0$ the saturation value, ν is the quantity of CO_2 adsorbed per unit mass of water ice, and ν_m the quantity of CO_2 adsorbed per unit mass of water ice for monolayer coverage. ν and ν_m are usually expressed as STP volume of gas (CO_2) per gram of adsorbent (H_2O), but they can also be given as the corresponding molecular ratio ($n_{gas}/n_{adsorbent}$). The BET constant c is approximately equal to $e^{(E_1-E_L)/kT}$, where E_1 and E_L are the heat of adsorption of the first layer and the heat of condensation, respectively. In Figure 3a we have plotted $\frac{p_{CO_2}}{\nu(p_{CO_2}^0 - p_{CO_2})}$ versus $\frac{p_{CO_2}}{p_{CO_2}^0}$ for the same experimental data shown in Figure 2b. A linear fit of the data presented in Figure 3a has been carried out in the range $0.01 < p_{CO_2}/p_{CO_2}^0 < 0.7$, as shown in Figure 3b. This relative pressure interval is consistent with the usual range in which the BET equation is relevant (Rouquerol et al., 1999). The parameters obtained from the fit are collected in Table 2.

[Figure 3]

[Table 2]

The specific surface area can be derived from ν_m by assuming an effective mean area for the adsorbed CO_2 molecules. We have taken 15.5 \AA^2 for this magnitude, a value which has been previously used by Sandford and Allamandolla and can be obtained from crystallographic data (Simon and Peters, 1980). With this assumption, a SSA of $39 \pm 15 \text{ m}^2/\text{g}$ for our ASW ice deposited at 95 K has been estimated.

The only other isotherm experiments that we are aware of, in which the concentration of the probe gas molecule in the solid is determined from IR spectra, are

those of Manca and co-workers (Manca et al., 2000; Martin et al., 2002, Manca et al. 2004). As in the present case, they employed the integrated absorbance of selected infrared bands of the IR spectrum of the ice to measure the amount of gas adsorbed. They found that this method gives similar results to standard volumetric experiments. Many other isotherm experiments based on volumetric measurements have been published in the literature, although the use of CO₂ as probe gas for ASW has not been reported so far, again within the limit of our knowledge. A study of CO₂ adsorption on water ice, carried out by Ocampo and Klinger (1982), was performed on hexagonal ice at temperatures between 195 K and 273 K. Ghormley (1967) made isotherm experiments on ASW with N₂, Ar, CH₄, and O₂. He obtained for N₂ isotherms a value of 241 m²/g at 77 K. Bar-Nun et al. (1987), using Ar as probe gas, found values from 86 m²/g at 77 K to 38 m²/g at 120 K. Mayer and Pletzer (1986) derived a SSA value of 43.84 m²/g at 77 K and of 40 m²/g at 113 K from N₂ adsorption measurements. Using also N₂, Schmitt et al. (1987) found SSA values between 258 and 35 m²/g. The infrared and volumetric co-measurements by Manca et al. (2003) were carried out on water ices deposited with Ar at 40 K, then annealed to 90 K to evaporate the Ar, and finally cooled down to the temperature of the experiment. They obtained SSA values of 102.4 m²/g for N₂ at 56 K and CO at 57 K, 85 m²/g for CH₄ at 73 K, 60.5 m²/g for Ar at 60 K, and 40.5 m²/g for Kr at 78 K. Their results show a remarkable dependence of the SSA with the probe gas, N₂ and CO giving the largest values both of the *c* BET constant and of the SSA. These observations are consistent with the existence of a specific interaction between the gas molecule and the ice surface leading to a higher affinity with the ice. Hydrogen bonding between ice and adsorbate should contribute to the high value of the adsorption energy, but there is probably another contribution, considering that N₂ and CO are the only molecules in the series studied that have a quadrupole moment. Since

CO₂ also has a quadrupole moment, its behaviour could be probably closer to that of N₂ or CO than to the rest of the molecules. However, other authors like Schmitt et al. (1987) obtained for N₂ a smaller SSA value than for Ar, in contradiction with the results of Manca et al. (2003). In a recent work Boxe et al. (2007) investigated the dependence of the SSA with water ice temperature using Kr adsorption experiments. They made also a careful study of the dependence of the SSA with the H₂O deposition rate and ice mass and concluded that the SSA is independent of both magnitudes, within their experimental error limits. They reported SSA values of $102.3 \pm 26.8 \text{ m}^2/\text{g}$ at 83.5 K, and $52.47 \pm 14.98 \text{ m}^2/\text{g}$ at 101 K.

Despite the disparity of methods and SSA values commented on in the previous paragraph there is a clear tendency to the decrease of SSA with growing ice temperature. The value of $39 \pm 15 \text{ m}^2/\text{g}$ at 95 K obtained in this work is consistent with some of the results previously mentioned, like those of Mayer and Pletzer (1986), Bar-Nun et al. (1987) and Boxe et al. (2007). In a previous publication (Gálvez et al. 2007), we provided a rough estimate of 140-280 m²/g for ASW ice at 85 K. This value is probably overestimated, since the crude assumptions made in that work do not allow for a proper distinction between mono- and multilayer adsorptions. In the present case, our SSA value arising from the application of the BET model corresponds to monolayers exclusively.

Comparison between co-deposition and sequential deposition methods

An inspection of the two panels in Figure 2 provides an immediate comparison between the two types of deposition employed in this work. In both cases, the measurements were performed at 95 K and with similar pressure ranges for CO₂ and

H₂O. The different ordinate scale reveals that there is always more CO₂ present in the co-deposited samples, with a $n_{\text{CO}_2}/n_{\text{H}_2\text{O}}$ ratio between nine times (at $p_{\text{CO}_2} \sim 1 \times 10^{-6}$ mbar) and 2.3 times (at $p_{\text{CO}_2} \sim 4 \times 10^{-5}$ mbar) larger. If the data in Figure 2a is plotted as a BET isotherm, the value for the surface active area is about three times higher than that evaluated for sequentially deposited experiments.

It is also interesting to remark that the maximum CO₂ pressure at which CO₂-ext starts to grow is smaller in the sequential deposition than in the co-deposition scheme (4.3×10^{-5} mbar versus 6.6×10^{-5} mbar, respectively).

Spectral band shape

In the following paragraphs the different band shapes of the CO₂ ν_3 band observed in both experiments will be discussed in an attempt to clarify the CO₂-H₂O interactions in these ice mixtures.

[Figure 4]

The ν_3 band adopts different shapes for sequential and co-deposition experiments at 95 K. Thinner and more symmetric bands are obtained in co-deposited samples. This band shape is typical of gas-phase spectra or of molecules isolated in a homogeneous solid matrix, which could be similar to our co-deposited samples, composed by CO₂ molecules trapped in a water surrounding.

In sequential deposition, the porous structure of the ASW formed is the key property in the process of gas adsorption. This porous structure is still under debate. From their isotherm experiments at 77 K Mayer and Pletzer (1986) concluded that ASW

was microporous. They compared their experimental isotherm with a non-porous standard isotherm, which they selected as the isotherm obtained from ASW deposited at 113 K. This empirical method, the so-called “ α -plot”, allows a semi-quantitative analysis of the microporosity of the material. If the sample is non-porous, adsorptions are similar on both materials (sample and reference) and the adsorbed amounts are proportional. Conversely, for a microporous sample, deviation from linearity at the beginning of adsorption is observed. In more recent works Manca and co-workers (Manca et al. 2000; Manca et al. 2002) have shown that the α -plots depend on the probe molecule used; this implies that the analysis has to be done with caution. In their studies, they claimed that their ASW samples, formed by a different deposition process than that used by Mayer and Pletzer, were non-microporous, arguing that the high SSA obtained was due to the formation of micro grains. In the last years, different studies have appeared in the literature concerning this topic. For example, Raut et al. (2007) have confirmed that the porosity of the ASW samples can be strongly altered by simply changing the angle of deposition in a collimated water vapour beam, in agreement with previous studies (Stevenson et al. 1999; Kimmel et al., 2001). Discrepancies in the different results found in the literature stress the fact that the porosity of the ASW is highly dependent on the way the ice is generated.

The broader bands observed in our sequential samples are symptomatic of CO₂ molecules in an inhomogeneous environment, undergoing intermolecular interactions of different strength, which results in IR absorptions spanning a wide frequency range. This could be the case for interactions occurring in a rough or macroporous surface, as opposed to the microporosity hypothesis in which a more homogeneous environment surrounding the CO₂ molecules is expected. The diameter of the cavity or macropore in the water ice is large enough to contain tens of layers of CO₂. Due to the constraint

given by the confinement to the shape of these cavities, the formation of a highly ordered structure of CO₂ is hindered. This fact induces broader IR bands, typical of an amorphous solid. The relatively small SSA obtained in this work (see Table 1) supports also the macroporous hypothesis. The macropores can also be understood as inter-grain cavities in the ice (Boxe et al., 2007).

In a typical sequential experiment, the intensity of the CO₂-int ν_3 band starts to decrease just after the CO₂ leak valve is closed. After a few minutes, which depend of the initial p_{CO_2} of the experiment, a constant integrated band value is observed, indicating that the desorption of CO₂ molecules from the ice has ceased. Further warming the ice to 105 K does not change the integrated band intensity. This band persists until the phase transition to the crystalline cubic structure, I_c , is nearly completed, at ~ 160 K, as was observed before (Jenniskens and Blake, 1994). Although the integrated band area remains constant, the shape of the band is significantly altered from 105 K to 140 K (see Fig. 4a). At ~ 131 K the ASW undergoes a phase transition from the low-density amorphous structure, I_{a1} , to a third amorphous form, I_{a2} , which precedes the crystallization to cubic ice, I_c , and coexists metastably with I_c in a wide range of temperatures (Jenniskens and Blake, 1994). During this phase transition, water molecules are rearranged and CO₂ molecules are free to move through the canals and pathways temporally formed during this process. As a result, CO₂ molecules are diluted inside the amorphous water structure in a way that, based on the band shape resemblance (see grey and solid black lines in Figure 4a), is closer to the one present in co-deposition experiments. Panel b) of Fig. 4 presents zoomed-in spectra in the ν_3 region of ¹³CO₂. At 140 K the band peak position has shifted from ~ 2280 to ~ 2275 cm⁻¹, which coincides with the frequency observed for co-deposited samples, and

supports the assumption that at 140 K the CO₂ molecular environment for sequentially deposited samples becomes similar to that in co-deposited samples at 95 K.

The *c* BET constant gives an idea of the strength of the CO₂-H₂O interaction (responsible for the formation of the monolayer) as compared to the CO₂-CO₂ interaction (responsible for the condensation process). From sequential experiments we have obtained a $(E_1-E_L)/k$ value of 186 ± 50 K. This value is consistent with the difference of 170 K between the heats of desorption of CO₂-H₂O (2860 ± 200 K) and CO₂-CO₂ (2690 ± 200 K) reported by Sandford and Allamandola (1990), but the coincidence is not conclusive due to the large uncertainties in the values of those magnitudes.

4. Conclusions.

The formation of CO₂-int in H₂O/CO₂ ice mixtures generated at 95 K by two different procedures, sequential deposition and co-deposition, has been studied in detail, yielding some quantitative results. These ice mixtures are abundant in different astrophysical bodies, and this study should help in the exploration of the physical properties of these objects. The main features obtained in this work are summarized below.

The mechanism of formation of CO₂-int depends on the procedure of deposition of the gases. In a co-deposited mixture, molecules of CO₂ are trapped in the amorphous water ice as it grows. The number of trapped molecules is not proportional to the CO₂ vapour pressure, but its growing rate decreases with increasing CO₂ proportion. The shape of the ν_3 IR band suggests that the CO₂ molecules in these samples are located in a homogeneous environment. On the other hand, in sequentially deposited mixtures, the

CO₂ molecules are filling the pores of the ASW, forming multilayers. For the CO₂ and H₂O vapour pressure ranges studied in this work, between nine and 2.3 times more CO₂-int is formed in co-deposited than in sequentially deposited samples.

From sequential deposition experiments, we have estimated for ASW at 95 K a SSA of 39 ± 15 m²/g, which falls within the widely spread literature data. This small SSA value, together with the band shape deformation observed for the CO₂ ν_3 band, favors the evidence that we have grown a macroporous ASW.

Annealing the sequentially deposited ice mixtures to 140 K entails a water phase transition. In this process the CO₂ molecules, located inside the pores in sequentially deposited samples, rearrange in the water structure reaching a CO₂ distribution equivalent to that in co-deposited samples.

The different signatures of the IR spectra of CO₂ trapped and adsorbed in amorphous water can be relevant for the interpretation of spectra of comet nuclei, when they become available. The heating of the nuclei when the comets pass by their perihelion may induce redistribution of the CO₂ molecules in the ice as described above, with consequent effects that can be detected by IR spectroscopy of sufficient quality. For instance, the spectra taken before and after impact on comet 9P/Tempel 1 by the Deep Impact probe, shown in Figure 3 of Crovisier (2006a), reveal a change in the region of the ν_3 band of CO₂, with a shoulder growing on the low-frequency side of the band. However, the quality of the spectra is not sufficient to allow for an unambiguous assignment of this feature. It can be expected that the data supplied in the present investigation could help to unravel observational data in the future.

Acknowledgments

This research has been carried out with funding from the Spanish Ministry of Education, Projects FIS2004-00456 and FIS2007-61686. O.G. acknowledges financial support from the same Ministry, “Juan de la Cierva” program.

References

- Bar-Nun, A., Dror, J., Kochvi, E., and Laufer, D. 1987. Amorphous water ice and its ability to trap gases. *Phys Rev B* 35(5), 2427-2435.
- Bar-Nun, A., Natesco, G., Owen, T. 2007. Trapping of N₂, CO and Ar in amorphous ice- Application to comets. *Icarus* 190, 655-659.
- Bernstein, M.P., Cruikshank, D.P., Sanford, S.A. 2005. Near-infrared laboratory spectra of solid H₂O/CO₂ and CH₃OH/CO₂ ice mixtures. *Icarus* 179, 527-534.
- Boxe, C.S., Bodsgrad, B.R., Smythe, W., Leu, M.T. 2007. Grain sizes, surface areas, and porosities of vapor-deposited H₂O ices used to simulate planetary icy surfaces. *J. of Colloid and Interface Science* 309, 412-418.
- Brunauer, S., Emmett, P.H., Teller, E. 1938. Adsorption of gases in multimolecular layers. *J. Am. Chem. Soc.* 60, 309-319.
- Buratti, B. J., 28 colleagues 2005. Cassini visual and infrared mapping spectrometer observations of Iapetus: Detection of CO₂. *Astrophys. J.* 622 (2), L149-152.
- Carrasco, E., Castillo, J.M., Escribano, R., Herrero V.J., Moreno, M.A., Rodríguez, J. 2002. A cryostat for low-temperature spectroscopy of condensable species. *Rev. Scientif. Inst.* 73, 3469-3473.

- Crovisier, J. 2006a. Recent results and future prospects for the spectroscopy of comets. *Molecular Physics* 104 (16-17), 2737-2751.
- Crovisier, J. 2006b. New trends in cometary chemistry. *Faraday Discuss.* 133, 375-385.
- Dartois, E. 2005. The ice survey opportunity of ISO. *Space Science Rev.* 119, 293-310.
- Draine, B. T. 2003. Interstellar dust grains. *Ann. Rev. A&A* 41, 241-289.
- Ehrenfreund, P., Boogert, A. C. A., Gerakines, P. A., Tielens, A. G. G. M., van Dishoeck, E. F.. 1997. Infrared spectroscopy of interstellar apolar ice analogs. *A&A* 328, 649-669.
- Ehrenfreund, P., Kerkhof, O., Schutte, W.A., Boogert, A.C.A., Gerakines, P.A., Dartois, E., d'Hendecourt, L., Tielens, A.G.G.M., van Dishoeck, E.F., Whittet D.C.B. 1999. Laboratory studies of thermally processed H₂O-CH₃OH-CO₂ ice mixtures and their astrophysical implications. *A&A* 350, 240-253.
- Gálvez, O., Ortega, I.K., Maté, B., Moreno, M.A., Martín-Llorente, B., Herrero, V.J., Escribano, R., Gutiérrez, P.J. 2007. A study of the interaction of CO₂ with water ice. *A&A* 472 (2), 691-698.
- Gerakines, P.A., Bray, J.J, Davis, A., Richey, C.R. 2005. The strengths of near-infrared absorption features relevant to interstellar and planetary ices. *ApJ* 620, 1140-1150.
- Gerakines, P.A., Schutte, W.A., Greenberg, J.M., van Dishoeck, E.F. 1995. The infrared band strength of H₂O, CO, and CO₂ in laboratory simulations of astrophysical ice mixtures. *A&A* 296, 810-818.
- Ghormley, J. A. 1967. Adsorption and occlusion of gases by low-temperature forms of ice. *J. Chem. Phys.* 46(4), 1321-1325.
- Grundy, W. M., Young, L. A., Young, E. F. 2003. Discovery of CO₂ ice and leading-trailing spectral asymmetry on the Uranian satellite Ariel. *Icarus* 162, 222-229.

- Hagen, W., Tielens, A. G. G. M., Greenberg, J. M. 1981. The infrared spectra of amorphous solid water and ice, I_c , between 10 K and 140 K. *Chem. Phys.* 56, 367-379.
- Hodyss, R., Johnson, P.V., Orzechowska, G.E., Goguen, J.D., Kanik, I. 2008. Carbon dioxide segregation in 1:4 and 1:9 $\text{CO}_2\text{:H}_2\text{O}$ ices. *Icarus* 194, 836-842.
- Jenniskens, P., Blake, D.F. 1994. Structural transitions in amorphous water ice and astrophysical implications. *Science* 265, 753-756.
- Kimmel, G.A., Stevenson, K.P., Dohnálek, Z., Smith, R.S., Kay, B.D. 2001. Control of amorphous solid water morphology using molecular beams. I. Experimental results. *J. Chem. Phys.* 114 (12), 5284-5294.
- Kumi, G., Malyk, S., Hawkins, S., Reisler, H., Wittig, C. 2006. Amorphous solid water films: transport and guest-host interactions with CO_2 and N_2O dopants. *J. Phys. Chem. A* 110, 2097-2105.
- Malyk, S., Kumi, G., Reisler, H., Witting, C. 2007. Trapping and release of CO_2 guest molecules by amorphous ice. *J. Phys. Chem. A* 111, 13365-13370.
- Manca, C., Roubin, P., Martin, C., 2000. Volumetric and infrared co-measurements of CH_4 and CO isotherms on microporous ice. *Chem. Phys. Lett.* 330, 21-26.
- Manca, C., Martin, D., Roubin, P. 2002. Spectroscopic and volumetric characterization of a non-microporous amorphous ice. *Chem. Phys. Lett.* 364, 220-224.
- Manca, C., Martin, C., Roubin, P. 2003. Comparative study of gas adsorption on amorphous ice: thermodynamic and spectroscopic features of the adlayer and the surface. *J. Phys. Chem. B* 107, 8929-8941.
- Manca, C., Martin, C., Roubin, P. 2004. Volumetric and infrared measurements on amorphous ice structure. *Chem. Phys.* 300, 53-62.

- Martin, C., Manca, C., Roubin, P. 2002. Adsorption of small molecules on amorphous ice: volumetric and FT-IR isotherm co-measurements. Part I. Different probe molecules. *Surface Science* 502-503, 275-279.
- Maté, B., Medialdea, A., Moreno, M. A., Escribano, R., Herrero, V. J. 2003. Experimental studies of amorphous and polycrystalline ices films using FT-RAIRS. *J. Phys. Chem. B* 107(40), 11098-11108.
- Maté, B., Gálvez, O., Martín-Llorente, B., Moreno, M.A., Herrero, V.J., Escribano, R., Artacho, E. 2008. Ices of CO₂/H₂O mixtures. Reflection-absorption IR spectroscopy and theoretical calculations. *J. Phys. Chem. A*. 112 (3), 457-465.
- Mayer, E. and Pletzer, R. 1986. Astrophysical implications of amorphous ice - a microporous solid. *Nature* 319(23), 298-301.
- Öberg, K.I., Fraser, H.J., Boogert, A.C.A., Bisschop, S.E., Fuchs, G.W., van Dishoeck, E.F., Linnartz, H. 2007. Effects of CO₂ on H₂O band profiles and band strengths in mixed H₂O:CO₂ ices. *A&A* 462, 1187-1198.
- Ocampo J. and Klinger, J. 1982. Adsorption of N₂ and CO₂ on ice. *J. of Colloid and Interface Science* 86(2), 377-383.
- Raut, U., Famá, M., Teolis, B.D., Baragiola, R.A. 2007. Characterization of porosity in vapor-deposited amorphous solid water from methane adsorption. *J. Chem. Phys.* 127, 204713.
- Roland, B., Devlin, J. P. 1991. Spectra of dangling OH groups at ice cluster surfaces and within pores of amorphous ice. *J. Chem. Phys.* 94, 812-813
- Rouquerol, F., Rouquerol, J., Sign, K. 1999. Adsorption by powders & porous solids. Academic Press, London.
- Sandford, S. A., Allamandola, L.J. 1990. The physical and infrared spectral properties of CO₂ in astrophysical ice analogs. *ApJ*. 355, 357-372.

- Schmitt, B., Ocampo, J., Klinger, J. 1987. Structure and evolution of different ice surfaces at low temperature. Adsorption studies. *Journal de Physique, Colloque C1*, 48(3), 519-525.
- Simon, A., Peters, K. 1980. Single-crystal refinement of the structure of carbon-dioxide. *Acta Crystallog. B36*, 2750-2751.
- Stevenson, K. P., Kimmel G. A., Dohnálek, Z., Smith, R. S., and Kay, B. D. 1999. Controlling the morphology of amorphous solid water. *Science* 283, 1505-1507.
- Strazzulla, G., Nisini, B., Leto, G., Palumbo, M.E., and Saraceno, P. 1998. Solid CO₂ towards NGC7538 IRS1. *A&A* 334, 1056-1059.
- Toon, O.B., Tolbert, M. A., Birgit, G. K., and Middlebrook, A. M. 1994. Infrared optical constants of H₂O ice, amorphous nitric acid solutions and nitric acid hydrates. *J. Geophys. Res.* 99 (D12), 25631-25654.
- Williams, D.A., Brown, W.A., Price, S.D., Rawlings, J.M.C., Viti, S. 2007. Molecules, ices and astronomy. *A&G* 48 (1), 25-34.

Table 1. Assignment and positions of CO₂ bands

| Assignment | Codeposited (this work 95K) | Codeposited (other works) | | | Pure CO ₂ (this work 95K) | Pure CO ₂ (other works) | | |
|---------------------------------------|-----------------------------------|------------------------------|-------------------|------------------|--|---------------------------------------|------------------|------------------|
| | | 15K ^H | 100K ^S | 15K ^B | | 80K ^H | 80K ^S | 60K ^G |
| $\nu_1+\nu_3$ | | 3703 | 3701 | 3702 | 3708 | 3708 | 3708 | 3708 |
| $2\nu_2+\nu_3$ | | 3593 | | 3592 | 3600 | 3600 | 3600 | 3600 |
| ¹² CO ₂ ν_3 | 2339 | | 2339 | 2341 | 2345 | | 2343 | 2343 |
| ¹³ CO ₂ ν_3 | 2275 | 2278 | 2277 | 2279 | 2282 | 2282 | 2282 | 2283 |
| ν_2 | 655 | 656 | 655 | 654 | 661 655 | 660 655 | 660 655 | 660 655 |

^HHodyss et al, 2008: H₂O/CO₂ 1:4 codeposited mixture, and pure CO₂

^SSandford and Allamandola, 1990: H₂O/CO₂ 1:5 codeposited mixture, and pure CO₂

^BBernstein et al, 2005: H₂O/CO₂ 1:5 codeposited mixture

^GGerakines et al., 1995: Pure CO₂ at 15 K and warm-up to 60K

Table 2.

BET constant c , ν_m expressed as molecular ratio ($n_{\text{CO}_2}/n_{\text{H}_2\text{O}}$), specific surface area SSA ($\text{m}^2 \text{g}^{-1}$), and net heat of adsorption $(E_I-E_L)/k$ (K).

| c | ν_m | SSA ^a | $(E_I-E_L)/k$ |
|------|---------|------------------|---------------|
| 7.06 | 0.0074 | 39 | 186 |

^a SSA calculated using an estimated cross-sectional area for CO₂ of 15.5 Å² (see text).

Figure 1. IR spectrum of a co-deposited H₂O/CO₂ mixture at 95 K in the full mid-IR range recorded.

Figure 2. Number of molecules ratio, $n_{\text{CO}_2}/n_{\text{H}_2\text{O}}$ vs partial CO₂ pressure. a) Co-deposited ice mixtures for three water pressure values. b) Sequentially deposited ice mixtures for ASW films of the specified growing rate and thickness.

Figure 3. a) BET representation of the same experimental data shown in Figure 2b. b) Zoomed-in region of $p_{\text{CO}_2}/p_{\text{CO}_2}^0 < 0.6$. Solid line: linear fit.

Figure 4. a) FTIR spectra of the ν_3 band of CO₂ in co-deposited and sequentially deposited ice mixtures with the same water amount. Gray solid line: Co-deposited CO₂/H₂O ice. The spectrum has been scaled by a factor (1/3) and offset for clarity. Dashed line: Spectrum taken after 14 minutes of exposure of a 370 nm ASW film to a CO₂ pressure of 3.2×10^{-5} mbar. Dotted line: spectrum taken after stopping the CO₂ flow and warming the ice to 105 K. Black solid line: Spectrum taken after warming the ice to 140 K. b) Zoomed-in spectra in the ν_3 region of ¹³CO₂.

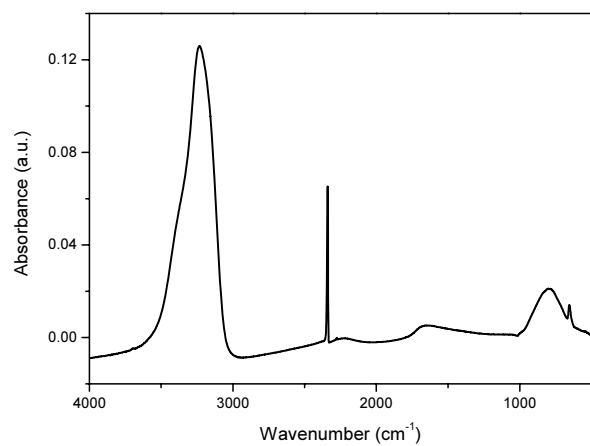


Figure 1

ACCEPTED MANUSCRIPT

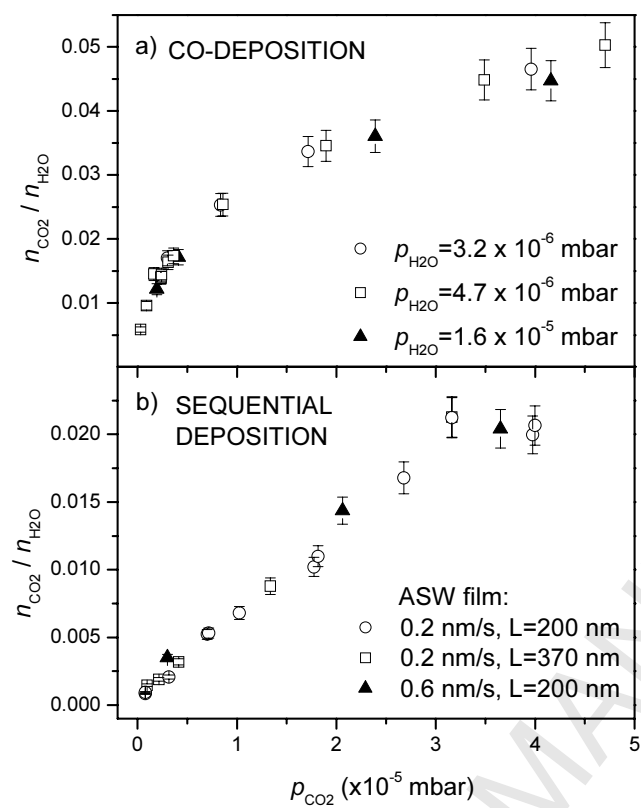


Figure 2

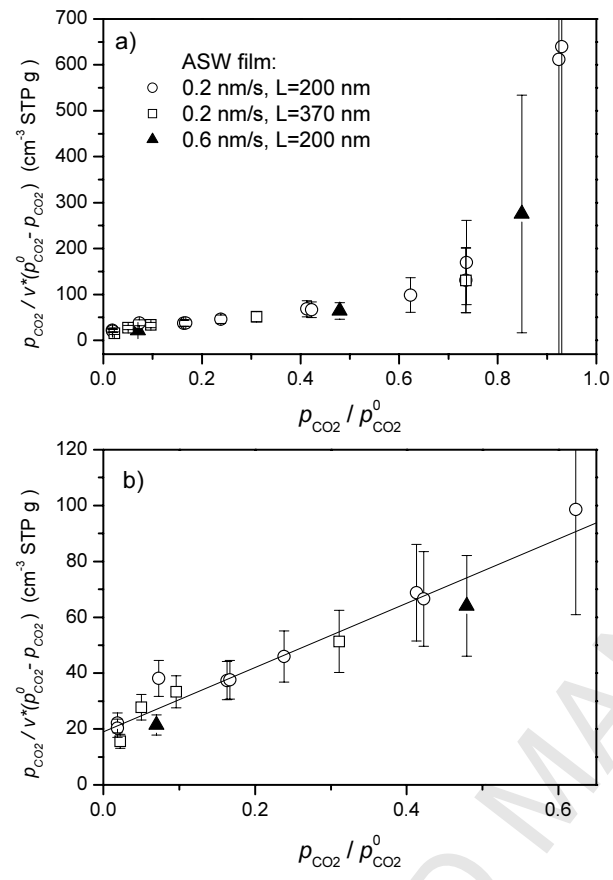


Figure 3

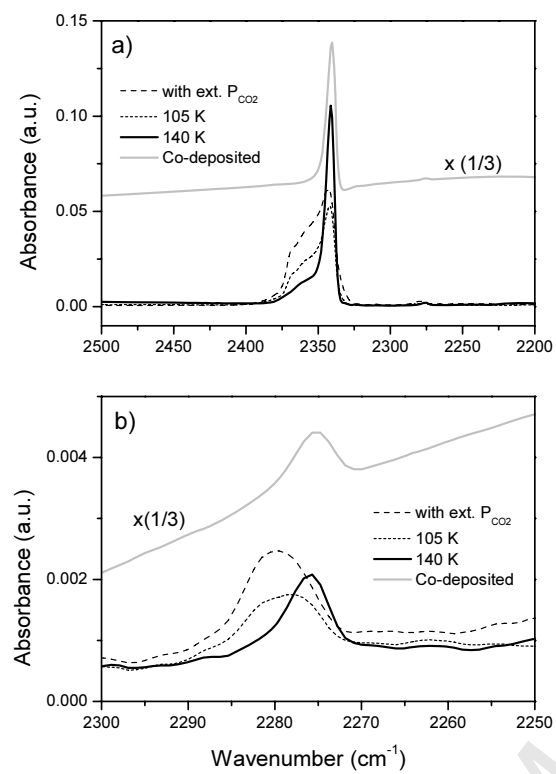


Figure 4